INVESTIGATION OF ALKALI OXIDES EFFECT ON VARIOUS PROPERTIES OF BOROSILICATE GLASSES

A dissertation submitted in partial fulfilment of the requirements for the award of degree of

Master of Physics

Submitted by

Rajni

301704025

Under the guidance of

Dr. Kulvir Singh

(Professor)

School of Physics and Materials Science

Thapar Institute of Engineering and Technology,

Patiala, Punjab (147001)

2019

Accomplished with the blessings

Of

God

&

Dedicated to my loving parents

Sh.Shiv Charan Dass and Smt.Darshna Devi

&

My lovely sisters and brother

CERTIFICATE

I hereby declare that the work which has been presented in the dissertation entitled ***"Investigation of different alkali oxides effect on properties of borosilicate glasses"*** *is an authentic record of my own work carried out for the partial fulfillment of the requirement for the award of the degree of Masters of Science in Physics at Thapar Institute of Engineering & Technology, Patiala (Punjab) under the guidance of* ***Dr. Kulvir Singh****, Professor, School of Physics and Materials Science. The matter submitted in this dissertation report has not been submitted in part or full for the award of any other degree.*

Date: 15 July 2019
Place: Patiala

Rajni
Rajni
(301704025)

This is to certify that the above statement made by the candidate is correct and true to the best of my knowledge and belief.

Dr. Kulvir Singh

Professor

School of Physics and Material Science

Thapar Institute of Engineering & Technology, Patiala-147004

Acknowledgements

At this momentous occasion of binding my thesis I would like to acknowledge the contribution of all those benevolent people, I have been blessed to associate with. All the data collection, theories would have failed to serve their purpose for me if blessings of God would not have joined hands with my efforts.

My first and foremost offering of thanks goes to my guide Dr. Kulvir Singh, School of Physics and Materials Science, Thapar Institute of Engineering and Technology, Patiala. He steered me through this journey with his invaluable advice, positive criticism, stimulating discussions and consistent encouragement. His meticulous attention towards my proceedings, his devoted time and his ideas has enabled me to make the project a success. His faith in me has always made me more confident. His blessings always made me optimistic. If I will stand proud of my achievements the undeniably he is main creditor. It had been my privilege to be under his tutelage. I would like to thanks Dr. O.P.Pandey, Prof. And Head, School of Physics and Materials Science for allowing me to use the facilities in Materials Research Lab and the opportunity to work on this project.

It gives me immense pleasure to express my special thanks to Mr.Savidh Khan, Mrs.Neetu Bansal and Mr. Gaurav Sharma, who always took keen interest in my work and for guiding me at various stages of my experimental work. Thank you, Mr.Savidh Khan for your kind helps from the core of my heart and for always being there.

I am also thankful to my dear friends Vandana Yadav, Anjali Mehta, Vikramjit Singh and my colleagues at the School of Physics and Materials Science are acknowledged for providing me a friendly atmosphere and encouraging me throughout this research.

Rajni

CONTENTS

LIST OF FIGURES

LIST OF TABLES

ABSTRACT

Three different alkali metal oxide containing borosilicate glasses are synthesized by melt quench technique. The as quenched glasses are characterized by x-ray diffraction, Fourier Transform infra-red spectroscopy, UV-Visible spectroscopy, Impedance spectroscopy and Vicker's hardness tester to check their applicability as substrate materials in thin film solar cell applications. The optical band gap is comparable to state of the art glasses i.e. 4.0 eV. The conductivity of the glasses is observed to be of order of 10^{-6} S/cm at 400°C. The hardness of the glasses decreases as K20S<Na20S<Li20S due to ionic bonding character increases with increasing atomic number.

Chapter-1 Introduction

1.1 History

Glass formation history was discovered in ancient Egypt in 3500 BC. According to archaeological evidences first glass was found in north Syria, Egypt [1]. Beads were the first glass object of the mid 3rd millennium BC. It was accidentally formed as consequence of metal workings or during faience production. It is a vitreous material made by a phenomenon related to glazing [2].

In India development of glass materials had begun in 1730 BC [3]. Across the Roman Empire glass materials have been recovered for their use in industrial, domestic and funerary contexts. In Anglo-Saxon period, glasses were extensively used in vessels, beads, jewellery and windows etc.

In 20th century, glasses are used as the building materials (such as laminated glasses, reinforced glasses and glass bricks). Modern technology became reality after the invention of glass. Replacing the copper wires with the glass optical fibres has revolutionised the telecommunication industry. It is encouraged detailed studies of glasses with non linear optical properties for communication. Usually glasses are very good insulators but they can be formed to have wide range of electrical properties. In addition to so many applications of glasses every walk of life, they can nowadays be used as sealant in energy technology [4]. Additionally, the glasses are also being used as electrolytes in fuel cells and battery applications.

1.2 Glasses

Glasses are amorphous solid that is generally hard. Glass exhibits glass transition temperature (T_g), below this temperature they have arbitrary arrangement of atoms and molecules. Glasses are also called "rapidly cooled liquids''. The most commonly known glass is soda lime glass, which is mainly constitutes silicon dioxide (SiO_2), lime (CaO), soda ash (Na_2O). The glass

properties are mainly influenced with the addition of modifiers (CaO, Na_2O, K_2O, Al_2O_3 etc) [4].

Silicate glasses can be used as building materials, window panes, wind screens, paper weights, beads, fibre optics etc due to their transparent nature. Due to their good optical properties (refractive index) they are used as prisms and optical lenses. With the addition of transition metals in glasses, colored glasses can also be obtained which can be used in manufacturing of art objects. The properties of the glasses could be tailored according to the need based applications.

1.3 Glass formation

The cooling of liquid from high temperature to room temperature can be done in two ways: rapid cooling and slow cooling as shown in Fig 1.1. . On cooling slowly, crystalline state arises as the molecules or atoms get sufficient time for arranging them in ordered (or periodic) manner. Secondly, during rapid cooling, molecules and atoms are randomly arranged, which leads to formation of glass. In both cases, change in volume and enthalpy is observed during cooling [5]. Crystallisation is a natural process which involves two step thermal processes. At first nucleation takes place and the secondly is crystal growth. During during rapid cooling, the atoms arrange them in random manner following the path1 (as shown in Fig 1.1) and forming glass. Due to discontinuous arrangement, the volume do not linearly depend upon temperature.

The cooling curve shows a change of slope at a specific temperature called transition temperature of glass (T_g). Transition temperature is decided by cooling rate [6,7]. The material obtained after the super cooled liquid has been transformed into non-crystalline solid is glass. Here, particles are unable to arrange them in particular way in this temperatrure range resulting in forming a glass [4].

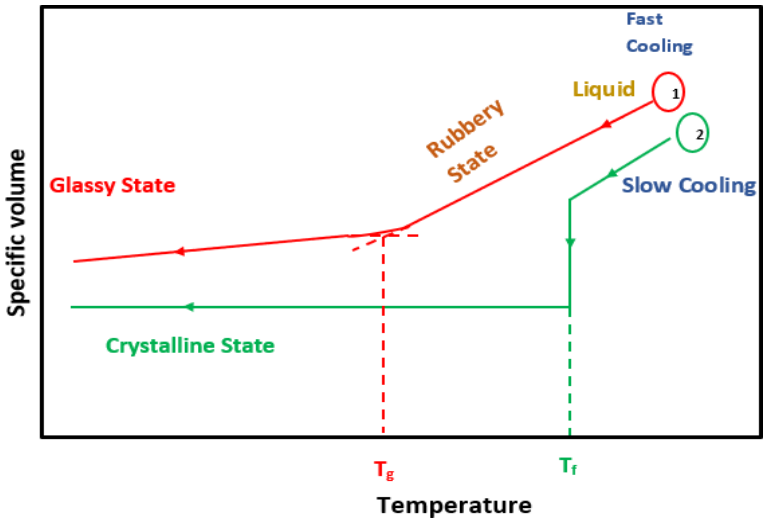

Fig 1.1 Temperature versus specific volume curves for glass and crystalline materials [8]

1.4 Components of oxide glasses

Glass formation depends on electronegativity and field strength of constituents. On the basis of this, there are three components that collectively form a glass. Those are network formers, intermediates and modifiers. The other components of glass oxides are colorants and fining agents.

1.4.1 Glass network former

They are the primary source of glass formation. It forms the matrix and the structure of the glass. SiO_2, B_2O_3 and P_2O_5 are the most commonly used glass formers. In addition to these, some are conditional glass formers like V_2O_5, As_2O_5, ZrO_2 etc. Glasses are predicted accordingly the glass former present in them for example, the glasses with silica as glass former are called silicate glasses. These substances are having small ionic radii, large charge and field strength lying in the range of 1.5-2.0/A° ,forms tetrahedral units. Glass formers generally have cation-oxygen bond strength more than 80 Kcal/mol and coordination number (CN) is generally small i.e.3 or 4 [4,9].

1.4.2 Network modifiers

The properties of glass materials are altered with the addition of modifiers to the glass composition. Oxides with low bond strengths do not become the part of network formers and

are known as modifiers. The bond strength of the modifiers generally lies in the range of 10 to 40 Kcal/mol and the CN varies from 4-10 [9]. They have large radius, small charge and very low electronegativity and field strength lies in 0.1-0.5/A° range. Some common glass modifiers are Na_2O, K_2O, Li_2O, CaO, BaO, MgO, HgO, SrO, ZnO, PbO etc [4]. The glass properties and its applications generally depend upon the choice of the modifiers. Network modifier occupies random positions in the glass network and breaks the network and leads to increase the number of the NBO's which alters glass properties [10,11].

1.4.3 Intermediates

These oxides can act both as network formers and modifiers. TiO_2, Al_2O_3, ThO_2, Bi_2O_3, BeO, ZnO_2, Y_2O_3, La_2O_3 and CdO are some examples of intermediates. The intermediates, generally, have electronegativity less than glass formers. Glass properties are modified after addition of intermediates to glass network [4,12].

1.4.4 Colorants and fining agents

As the name suggests colorants are those which controls colour to the glass. Mostly the transition metal oxides (3d elements) or 4f rare earths (for e.g. Cu, Fe, Au, Ag Mn etc) are used as colorants. To remove the bubbles from the glass melts fining agents are added to the glass batches during glass formation. Arsenic oxide, NaCl, CaF_2 etc are used as fining agents. Both of them are added in very little amount and therefore they donot alter the properties of the glass [4].

1.5 Types of glasses

On the basis of composition and formers the glasses are categorized into following categories:

1.5.1 Silicate glasses

The most studied glasses are the silicate glasses and their fundamental constituent is silica (SiO2). The basic structural unit for silicate glass is tetrahedral. Silicate glasses posses

attractive and some interesting properties such as low electrical conductivity, low thermal expansion, high corrosion resistance, chemically stable low non linear refractive index, good durability and high tensile fracture strength [13]. Silicate glasses are more expensive than soda lime glass, that is why soda lime glass is more widely used than silicate glass [14].

1.5.2 Borate glasses

The glass systems which have B_2O_3 as the network forming unit are known as borate glasses. Borate glasses have lower T_g as compared to silicate glasses [15,16]. Borate glasses can be used for energy storage applications and they have fast ionic conductive properties. With the addition of the heavy metal oxide the density of the borate glasses increases. These glasses are having high viscosity and good optical properties [4]. Adding alkali oxides to the borate glasses results in formation of the NBO's , which increases as the amount of alkali oxide increases.

1.5.3 Phosphate glasses

The main component of these glasses is P_2O_5, they have complex structure and poor chemical durability. They are commonly used in semiconductor technology because of their negative temperature coefficient of resistance and time independent dc conductivity. These glasses exhibit interesting magnetic and electrical properties. These glasses are used in making gratings in polystyrene-fibres [17].

1.5.4 Chalcogenide glasses

Glasses comprising selenium, sulphur and VI group elements are referred as chalcogenide glasses. These glasses can also be formed from IV and V group elements. They are generally semiconducting by nature and possess electronic conductivities ranging from 10^{-3} $ohm^{-1}cm^{-1}$ to 10^{-13} $ohm^{-1}cm^{-1}$. These glasses are widely used in optical applications as they have strong tendency to absorb the radiations in visible region. These glasses have applications in amplifiers and lasers after adding rare earth metals in them as modifiers [4,18,19].

1.5.5 Halide glasses

Halide glasses are generally based on inorganic fluorides of heavy metals. As compared to silica glasses, in general halide glasses have low T_g than silica glasses and are comparatively less stable. They are used in windows, lenses. They exhibit fewer applications because of their low mechanical strength, low chemical durability and highly thermal shocks sensitive.

1.5.6 Metallic glasses

It is usually an alloy with the disordered atomic scale structure. These glasses contain metal elements instead of oxides. They obtain their metallic properties from the melt. These glasses are formed by extreme rapid cooling process and are stronger than the crystalline metals. Mostly metals are crystalline in nature but the metallic glasses are amorphous and unlike other glasses they are good electrical conductors. Metallic glasses possess extra ordinary properties like strength, elasticity, toughness etc [20].

1.6 Properties of glasses

The basic properties of the glasses are related to liquids, for example transparency is the characteristic of liquid rather than solids. The other important properties are explained below:

1.6.1 Physical and structural properties

The two main physical properties of glasses are density and molar volume. Density of glasses increases with addition of the glass modifiers as they occupy the interstitial sites. The addition of alkali metals to silicate glasses generally increases density [4]. Density of the glass samples also depends upon their processing conditions, cooling rate and hence, glasses are obtained with different densities. The behaviour of glass is estimated by density and molar volume (volume of 1 mole of structural groups). Both depend on the composition of glass.

1.6.2 Optical properties

Glasses have excellent optical properties and hence have many applications like in window

panes, lenses, prisms, communication technology etc. These applications are mainly based on refractive index, transmission, absorption and reflection. The optical properties are affected by the creation of the NBO's and the glass composition. The refractive index increases with amount of NBO's. Refractive index also depends upon the cooling rate i.e. glasses formed with faster cooling rate have high value of refractive index and glasses with low cooling rate have low value of refractive index [21].

1.6.3 Electrical properties

Glasses are generally ionic conductors by nature and are widely used in solid state batteries as electrolytes. Conductivity of glasses can be altered by adding modifiers. Pure glass (silica glass) is insulator in nature. Glasses containing the transition metal oxides possesses the electronic conductivity and this is influenced by existence of transition metal ions [22,23]. The conductivity of the glasses depends upon the size, nature and concentration of hopping ion. Dielectric properties depend on composition, temperature and frequency. Generally, dielectric constant of glasses depends directly on temperature and inversely on the frequency.

1.6.4 Mechanical properties

Glasses are hard materials. As a result, environmental factors are responsible for their fracture behaviour and not the inherent strength of the bonds forming the vitreous network. The fracture toughness strength of glasses differs with previous surface treatment, chemical surroundings, and therefore the technique used to measure the material strength. Being the brittle materials, glasses are also quite receptive to failure due to thermal shock [24]. Other mechanical properties of glasses are material in-built. The coefficient of elasticity (E) is ruled by the structure of the network and by the individual bonds within the material. The hardness of depends on the strength of individual bonds.

1.7 Objective

1. To synthesise alkali oxide based borosilicate glasses with composition $60SiO_2$-$5B_2O_3$-$15CaO$-$20R_2O$ (where R = Na, Li, K).

2. To study their structural, optical, dielectric and conducting properties using various characterisation techniques.

References

1. F. Subial, F. Jessica, C. Ralph, L. Holloway and H.S. Terrace, J. Mater. Sci., 305 (2004), 407.
2. W.M. Allen, B.F. Sansom, C.F. Drake and D.C. Davies, J. Ceram. Engg. & Sci. Proceed, 2 (1978) 73.
3. W.M. Allen, B.F. Sansom, P.T. Gleed, C.B. Mallison and C.F. Drake, J. American Ceramic Society, 55 (1984) 115.
4. J. E. Shelby, "Introduction to Glass Science and Technology" 2nd edition, The Royal Society of Chemistry, U. K. (2005).
5. R. J. D. Tilley, Crystal and Crystal Structures, Chichester, UK (2006).
6. R. Hu, C. Yan, L. Xie, Y. Cheng, D. Wang, Int. J. Hydrogen Energ., 36 (2011) 64.
7. S. Banerjee, A. K. Tyagi, Functional Materials: Preparation, Processing and Applications 1st sedition, Elesvier Insights, USA (2012).
8. P. Murugasen, S. Sagadevan, D. Shajan, Int. J. Chem. Sci., 13 (2015) 693.
9. W. Vogel, "Glass Chemistry" 2nd Edition, (1994) 42.
10. S. Singh, K. Singh, J. Mol. Struct., 1081 (2015) 211.
11. S. K. Arya, K. Singh, J. Non-Cryst. Solids., 414 (2015) 51.
12. W. F. Smith, Principles of Materials Science and Engineering 3rd edition, McGraw-Hill USA (2012).
13. S. Singh, K. Singh, J. Non-Cryst. Solids., 386 (2014) 100.
14. L. L. Hench, J. Am. Ceram. Soc., 74 (1991) 1487.
15. W. A. Pisarski, T. Goryczka, B. W. Dus, M. Plonska, J. Pisarska, J. Mater. Sci. Eng., 122 (2005) 94.
16. S. G. Motke, S. P. Yawale, S. S. Yawale, J. Bull. Mater. Sci., 25 (2002) 75.
17. Y. Shioya, M. Maeda, J. Electro. Chem. Soc., 133 (1986) 1943.

18. M. A. Afifi, H. H. Labib, M. H. Fazary, M. Fadel, Appl. Phys. A, 55 (1992) 167.
19. Y. Shpotiuk, V. Baltiska, Journal of physics: Conference series, 289 (2011) 1.
20. B. W. An, E. J. Gwak, K. Kim, Y. C. Kim, J. Jang, J. Y. Kim, J. U. Park, Nano Lett., 16 (2015) 471.
21. T. Honma, R. Sato, Y. Benino, T. Komatsu, V. Dimitrov, J. Non-Cryst. Solids, 272 (2000) 1.
22. M. E. D. Mohamed, S. M. Salem, I. Kashif, J. Mater. Sci., 10 (1999) 279.
23. S. K. Arya, S. S. Danewalia, K. Singh, J. Mater. Chem. C, (2016) 3328
24. R.S. Gedam, D.D. Ramteke, J. of phy. & chem. of sol., 74 (2013) 1399.

The aim of this section is to present the work done so far in the study of different properties of alkali ion doped silicate glasses done till now.

Verhoef *et al*. [1] studied the dielectric properties of lithium borate glasses with composition $(B_2O_3)_{1-x}$-$(Li_2O)_x$ (where x varies from 0.20 to 0.45) in the frequency range of 5MHz to 10GHz. It was observed that the formation of NBO clusters greatly influences the diffusion of lithium ions, which starts diminishing at lithium oxide concentration x=0.4. Further, it was concluded that the conductivity exponent (s) depends upon temperature as well as composition. Lower values of 's' results in higher rate of hops and hence higher d.c. conductivity.

Eldin *et al.* [2] observed the variations of conductivity of soda-silica glasses doped with CaO or Al_2O_3. It was noted that as the sodium content increases in these glasses, electrical conductivity increases. The dc conductivity for the samples containing substituted CaO and Al_2O_3 was smaller than those containing soda alone. The conductivity of samples is related to the mobility of the alkali ions. Conductivity of glasses is related to the change in composition which affects the internal structure and hence ability of alkali ion to conduct electricity.

Serra *et al.* [3] extensively studied the multi-component glasses containing Na_2O-CaO-P_2O_5-K_2O-MgO-B_2O_3-SiO_2 systems using x-ray photo spectroscopy (XPS) and Fourier transform infra-red spectroscopy (FTIR). As the alkali oxides are introduced into silica network, the local symmetry and electronic density gets modified. As a consequence there is shifting of IR peaks related to bridging oxygen (BOs) stretching vibrations (Si-O-Si). Also the presence of Si-O-NBO groups is investigated.

Galhot *et al.* [4] prepared two series of glasses with composition xZnO-(0.30-x)Li_2O-0.7Bi_2O_3 and xZnO-(30-x)Na_2O-70Bi_2O_3 ($0 \leq x \leq 20$) to study their different properties. In both cases, density of the samples increases with increase in amount of ZnO. The optical band gap

is inversely related to the ZnO content and lies between 2.18 eV-2.38 eV. The sample with Na has the highest optical band gap i.e. 2.38eV as it has less number of NBO's in it. It was observed that conductivity of sample series with Na is less than that with Li because Li ions can easily move in glass network as compared to Na ions.

Grandjean *et al.* [5] synthesised SiO2-B2O3-Na2O glass system over wide range of composition to study ionic diffusion. Using differential thermal analysis (DTA) it was noted that below T_g Arrhenius law characteristics are followed for the static conductivity, which arises due to long range ionic displacements. In these samples, the activation energy (E_a) of static electrical conductivity is corelated with the coordination number (CN) of boron. The activation energy is found to vary from 0.65eV-0.91eV. These values are found to be in agreement with the Na_2O-B_2O_3 and Na_2O-SiO_2 glass systems.

Two groups of borosilicate glasses are prepared by melt quench technique one of them exhibit fixed SiO_2, Al_2O_3, B_2O_3, CaO amounts and introduced various alkali metal oxides (Na_2O, K_2O, Li_2O). On the other hand, second group is with fixed SiO_2, Al_2O_3, B_2O_3, Na_2O, Li_2O content and different metal oxides (CaO, MgO, ZnO). It was observed that both the groups are having low dielectric constant ranging from 5-6 and loss (10^{-2}-10^{-3}), higher values of electric resistivity ($10^{12\text{-}13}\Omega$ cm) and low temperature firing properties [6]. [**Wang** *et al.*]

Smedskjaer *et al.* [8] compared the hardness of two series of glass samples that are $68SiO_2$-$8Na_2O$-$1Fe_2O_3$-23MO (M=Mg, Ca, Sr, Ba) and $68SiO_2$-23CaO-$1Fe_2O_3$-$8R_2O$ (R = Na, K, Rb, Cs). The network modifying ions affects the hardness of two series differently. The variation of hardness with ionic radii is opposite in both cases i.e. for alkali ions, hardness increases with increasing ionic radii and opposite for alkaline earth ions.

Zaid *et al.* [9] studied the physical properties of ZnO doped soda lime silicate glasses having ZnO_x-$SLS_{(1-x)}$ composition (where x= 0, 0.05, 0.1, 0.2, 0.3, 0.4). Broad halos were observed in XRD pattern of samples. The density and molar volume of glasses increases with

concentration of ZnO. The increase in molar volume is due to changes in glass structure with addition of ZnO. The optical band of glasses decreased from 3.20 eV to 2.32 eV with increasing ZnO content.

Kaur *et al.* [10] studied how the modifiers effects different properties of $XO\text{-}SiO_2\text{-}B_2O_3\text{-}La_2O_3$, (X=Mg, Ca, Sr, Ba) composition glasses. With the replacement of heavy metals the NBO's increases in the glass samples leading to decrease the optical band gap and increase Urbach energy. Also, as the heavy metal ions are replaced the bands in FTIR spectra shifted slightly to lower wavelengths. Sample with Ba has higher values of refractive index, optical basicity, oxide ion polarisability and the sample with Mg has highest value of hardness and fracture toughness value which corresponds to high Mg-O bond strength.

He *et al.* [11] synthesised glasses with composition $81SiO_2\text{-}12B_2O_3\text{-}(6\text{-}x)Na_2O\text{-}0.50CaO\text{-}0.50Al_2O_3\text{-}xLi_2O$ (x=0, 0.5, 1, 1.5, 2.0 moles of Li2O). FTIR spectroscopy reveals that the effect of concentration of Li_2O on viscosity is directly related to glass structure. The viscosity of the samples decreases until content of 1 mol of Li_2O is reached. This abnormal behaviour is due to high ionic field strength of Li_2O which weakens the Si-O-Si bond strength. The peak at 1400 cm^{-1} assigned to stretching relaxation of B-O bond of $[BO_3]$ units becomes stronger as Li_2O content increases, concluding the weaker ability to provide free oxygen of Li_2O compared to that of Na_2O.

Aboutaleb *et al.* [12] prepared glass samples with composition $(95\text{-}x)B_2O_3\text{-}(x)Al_2O_3\text{-}5LiO_2$ (x=5, 10, 15, 20, 25) to study the effect of LiO_2 on the physical and thermal properties of borate glasses. It was noted that the density of glasses increases with increasing lithium content and hence the molar volume decreases. The addition of LiO_2 has greatly affected the structure of borate glasses. As the LiO_2 increases (at x= 10, 15) there is termination of phase separation but at x=20 phase separation re-occurred. The electrical permittivity also increases with increase in lithium content.

Jha *et al.* [13] studied the structural and optical properties of the glass samples with composition $55SiO_2$-$10K_2O$-$(35-x)CaO$-$xMgO$ ($0 \leq x \leq 30$). The as quenched samples were analysed using XRD, FTIR and UV-Visible spectroscopy. It is observed that glasses with higher MgO content shows tendency of phase separation. As CaO is replaced with MgO, there is decrease in density. Some weak bands near 1393, 1461 and 1530 cm^{-1} are observed in FTIR spectra corresponding to Ca/Mg-O-H bonding. Optical band gap ranging from 3.42 eV-3.72 eV is found indicating that the glass samples can be used in non-linear optic applications.

Arya *et al.* [14] investigated the various properties of $(70-x)SiO_2$-xNa_2O-$15CaO$-$10Al_2O_3$-$5TiO_2$ ($10 \leq x \leq 25$) glasses. The density of glass samples increases with increase in Na_2O content and molar volume follows opposite trend. The activation energy values increases with decrease in sodium content and ranges from 32.6 to 82.2 kJ/mol. The glass with highest sodium content exhibits highest band gap value that is 4.52 eV. FTIR spectra reveal that there is shifting of peaks towards the higher wavenumber as the silica concentration increases in sample. This may be due to change in crystalline field effect on increasing silica concentration, which leads to strengthening of stretching modes and weakening of vibrational modes.

Singh *et al.* [15] prepared glasses with composition $55SiO_2$-$30B_2O_3$-$xLiO_2$-$(15-x)Y_2O_3$ (x=0, 5, 10, 15) to study their structural, physical, optical and conducting properties. It was observed that except for x=0, all the samples are amorphous. The optical band gap of the samples increases with increasing Li content in the samples. The optical band gap values lies between 3.64 eV – 3.90 eV i.e. in insulator range. The conductivity is of order of 10^{-6} S/cm at 620^0C and the E_a is 1.20 eV, concluding that glasses are ionic conductors in nature.

Barlet *et al.* [16] studied the hardness and toughness of sodium borosilicate glasses with change in their chemical composition via Vickers's indentation. It was observed that higher

hardness values were obtained for those glasses which have more network formers in them. Glasses with low sodium content possess high network connectivity and low value of Poisson's ratio and vice versa. Increase in alkali content in glasses predominates the shear flow process. As with increase in sodium concentration shear flow increases, stresses during loading and unloading favours lateral-radial cracks. Hence, it was concluded that the fracture toughness varies indirectly with Poisson's ratio.

Neyret *et al.* [17] investigated the alkali ion transport in SiO_2-B_2O_3-M_2O glasses (M=Li, Na, K or Cs) using impedance spectroscopy. It was shown that as the size of alkali ions increases, the glass network expands the binding forces between alkali ions and NBO's gets weakened and especially T_g and electrical conductivity changes. Independent of alkali ions present, the conductivity was shown to follow Arrhenius law. The greater hopping distance for alkali diffusion and high activation energy of diffusion is attributed to decrease in field strength from Li to Cs.

Yadav *et al.* [18] observed the structural, optical and electrical properties of $0.70TeO_2$-$(0.30-x)Na_2O$-xK_2O ($0 \leq x \leq 0.3$) glasses. Presence of alkali ions affects the structural units of TeO_2. The optical band gap of these samples is found to be in range 3.43-3.74 eV. With the increasing amount of K_2O, the density, molar volume, optical basicity, refractive index values were found to increase, whereas Urbach energy decreased. Also with the increasing K_2O content, the conductivity of samples increases.

Gundale *et al.* [19] prepared glasses with composition $40Li_2O$-$(60-x)[(2/3)B_2O_3$-$(1/3)\ SiO_2]$-xLi_2SO_4 (x=0, 5, 10, 15 mol%) using melt quench technique. The conductivity of glass samples increases with increase in Li_2SO_4 content. The maximum value of ionic conductivity was found to be at x=15 i.e. 4.08×10^{-4} S cm^{-1} at 523K. Density and T_g decreases with the addition of Li_2SO_4 indicating the weakening of glass structure and expansion of network. This leads to increase in conductivity.

Dagdale *et al.* [20] prepared glass samples with composition $3Li_2O$-$2K_2O$-$5B_2O_3$ via melt quench technique. The amorphous nature of the samples was confirmed using the x-ray diffraction technique. The UV-Visible spectroscopy is used to calculate the optical band and was found to be 6.3 eV.

Kaur *et al.* [21] synthesised $(60-x)SiO_2$-$15CaO$-$10Al_2O_3$-$5TiO_2$-$(10+x)Na_2O$ (x = 0, 5, 10, 15) glass samples by melt and quench technique. It was found that conductivity increases with frequency and lies in range of 10^{-5}-10^{-3} S/m. Both conductivity and dielectric constant rise with increase in temperature and sodium content. The conductivity obeys super linear power law.

Hanumantharaju *et al.* The glasses with $(100–x)(33.35Li_2O$-$66.65B_2O_3) – xGd_2O_3$, in which x = 0, 0.5, 1.0, 1.5 and 2 mol% compositions were prepared. The electrical conductivity and dielectric properties were observed in temperature range of 393-573 K and frequency range 100 Hz – 5 MHz. The dc conductivity is found to be maximum for x=0 ,i.e. 1.7516×10^{-6} S/cm. The Activation energy is found to lie in range of 0.809-0.903 eV.

Salinigopal et al. Alkaline earth based glasses of composition $35AO$-$50B_2O_3$-$15SiO_2$ (A = Ba, Ca, Sr) was prepared by melt quench technique. The density of these samples varies from 3.16 – 3.84 g/cc. Microhardness of these glasses was found to be high (6.18-7.17 GPa) which tells higher bond strength of alkaline earth borosilicate glass. The coefficient of thermal expansion is found to be of order of $10^{-6}/^0C$

From the literature discussed above, it was observed that the presence of different alkali oxides or same alkali oxide with different concentration greatly affects the properties of the glasses. Hence, it can be concluded that the structural, optical, dielectric and conducting properties are greatly influenced by the composition of the glass system and also the content and type of alkali ions present in the glasses. So in next section we discussed about the glass system effect of different alkali oxides on various properties of glass system. The motivation

of the present study is to study effect of different alkali oxides with fixed amount of all other four components. These glasses can be used as substrate in solar cell applications. Before using them in high end applications, their physical, structural, conducting and optical properties can give an essential background for these applications.

References

1. A. Verhoef, H. Hartog, Solid State Ionics, 68 (1994) 305-315.
2. F. Eldin, N. Alaily, Mater Chem Phys., 52, (1998), 175-179.
3. J. Serra, P. Gonzalez, S. Liste *et al.*, J. Non-Cryst Solids, 332 (2003) 20-27.
4. P. Galhot, V. Seth, A. Agarwal *et al.*, Radiat Eff Defect S., 159 (2004) 223-231.
5. A. Grandjean, M. Malki, C. Simonnet, J. Non-Cryst Solids, 352 (2006) 2731-2736.
6. Z. Wang, Y. Hu, H. Lu *et al.*, J. Non-Cryst Solids, 354 (2008) 1128-1132.
7. M. Smedskjaer, M. Jensen, Y. Yue, J. Non-Cryst Solids, 356 (2010) 893-897.
8. M. Zaid, K. Matori, S. Aziz *et al.*, Int. J. Mol. Sci., 13 (2012) 7550-7558.
9. G. Kaur, O. Pandey, K. Singh, J. Non-Cryst Solids, 358 (2012) 2589-2596.
10. F. He, C. Ping, Y. Zheng, Physcs Proc., 48 (2013) 73-80.
11. D. Aboutaleb, B. Safi, Int. J. Chem. & Mol. Eng., 9 (2015) 425-428.
12. P. Jha, K. Singh, Silicon, 8 (2015) 437-442.
13. S. Arya, B. Kaur, G. Kaur *et al.*, J. Therm Anal Calorim, 120 (2015) 1163-1171.
14. S. Singh, G. Kalia, K. Singh, J. Mol. Struct., 1086 (2015) 239-245.
15. M. Barlet, J. Delaye, T. Charpentier *et al.*, J. Non-Cryst Solids, 417-418 (2015) 66-79.
16. M. Neyret, M. Lenoir, A. Grandjean *et al.*, J. Non-Cryst Solids, 410 (2015) 74-81.
17. A. Yadav, P. Jha, S. Murugavel *et al.*, Solid State Ionics, 296 (2016) 54-62.
18. S. Gundale, V. Behare, A. Deshpande, Solid State Ionics, 298 (2016) 57-62.
19. S. Dagdale, G. Harde, V. Pahurkar *et al.*, Res. J. Chem. Sci., 7 (2017) 30-32.
20. B. Kaur, K. Singh, O. Pandey *et al.*, J. Non-Cryst Solids, 465 (2017) 26-30.
21. N. Hanumantharaju, G. Sriprakash, V. Gowda, J. Non-Cryst Solids, 52 (2019) 103-111.
22. M. Salinigopal, N. Gopakumar, P. Anjana, Silicon, (2019).

Chapter-3 Experimental details

In this chapter we will discuss about the sample preparation and different characterization techniques used to investigate their change in properties.

3.1 Sample preparation

Glasses with composition $60SiO_2$-$5B_2O_3$-$15CaO$-$20R_2O$ (where R = Na, Li, K) are synthesized using melt quench technique. Appropriate amounts of the high purity oxides (SiO_2, B_2O_3, CaO, Na_2O, K_2O, Li_2O) were mixed in an agate mortar pestle for approximately 2hours (h) in acetone medium. The samples were then put in re-crystallized alumina crucible and then melted in programmable high resistance electric furnace at 1550°C at the heating rate of 5°C/min. The furnace was held at different temperatures for 30 min after every one hour. To attain homogeneity the melt was held at same temperature (1550°C) for 2hrs. The melts are quenched in air between two thick copper plates. The samples are labelled accordingly which alkali ion is present, as Na20S, K20S, Li20S. The density (ρ) of as-quenched samples was calculated at room temperature in xylene using the standard Archimedes principle. Further the molar volume (V_m) is calculated using the formulae $V_m = M/\rho$ (M is the molecular weight).

The crushed powder samples were characterized by X-ray diffraction technique using PANalytical X'Pert Pro diffractometer in the diffraction angle range of 2Θ=10-80°, with Cu-K_α radiation (λ=1.54A°). The infrared spectra of the as-quenched samples were recorded using Perkin Elmer-Spectrum-RF-1 FTIR spectrometer at room temperature in the range of 200-4000cm^{-1}. The optical reflectance spectra of the powdered samples were recorded in the wavelength range of 200-800nm at room temperature using double beam UV-Vis spectrophotometer. H). The dielectric measurements of Pt coated pellets were taken on Solartron analytical impedance analyzer (Model: SI 1260) in the frequency and temperature range of 102-106 Hz and 50-500 °C, respectively.

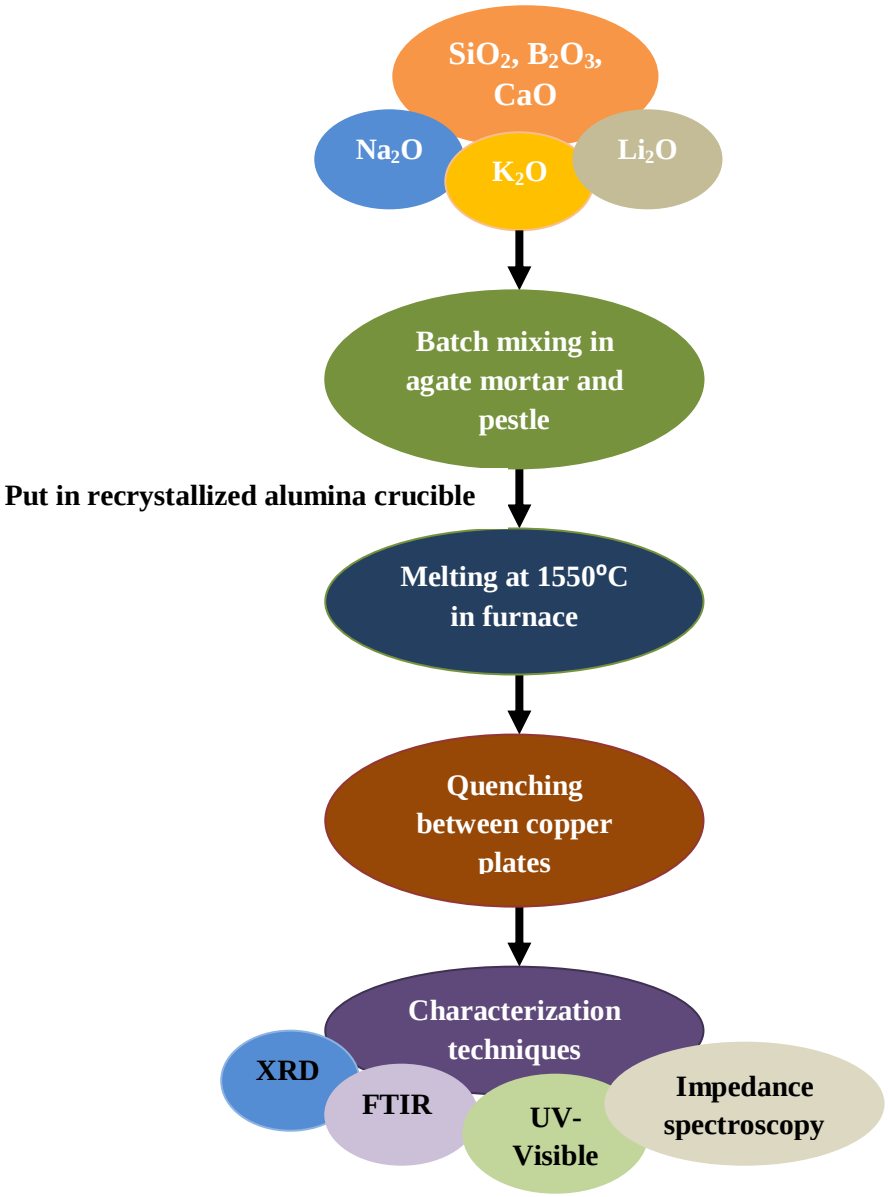

Fig 3.1 Flow chart representing the sample preparation process

3.2 Characterization Techniques

3.2.1 Physical Parameters

The density of prepared samples was calculated using standard Archimedes principle.

$$\rho = \frac{W_a \times \rho_x}{W_x} \tag{3.1}$$

Where, ρ is the calculated density, W_a and W_x is the weight of glass sample in air and xylene respectively. ρ_x is the density of xylene (0.863 g/cc). The molar volume can be measured using the formula given as:

$$V_m = \frac{M}{\rho} \tag{3.2}$$

where, V_m is the molar volume and M is the molecular mass of the glass.

Further the inter-ionic concentration (N), ionic radii (R) and polaron radii (r_p) are calculated using following formulae:

$$N = \frac{6.023\times10^{23}\times(mol\%\ cation)\times valency}{V_m} \tag{3.3}$$

$$R = \left(\frac{1}{N}\right)^{\frac{1}{3}} \tag{3.4}$$

$$r_p = \frac{R}{2}\left(\frac{\pi}{6}\right)^{1/3} \tag{3.5}$$

3.2.2 X-Ray diffraction (XRD)

X-ray diffraction technique provides data related to crystal structure, chemical composition and physical properties of the materials. X-rays are diffracted from crystal atoms at different angles and with different intensities and the measurement of these angles and intensities can be used to calculate the electron density within the crystal. X-rays are the form of electromagnetic radiations that have short wavelength and high energy. X-rays have wavelength of the order of atomic spacing within the crystal. The crystal planes acts as diffraction grating to the incident x-rays and hence when the x-rays are incident on any material it gets diffracted from the crystal planes as shown in Fig (3.2). The Bragg's law, is given as:

$$2d\sin\theta = n\lambda \tag{3.6}$$

Where, d is the interplanar spacing, Θ is the angle of incidence, λ is the wavelength of incident beam and n is order of diffraction.

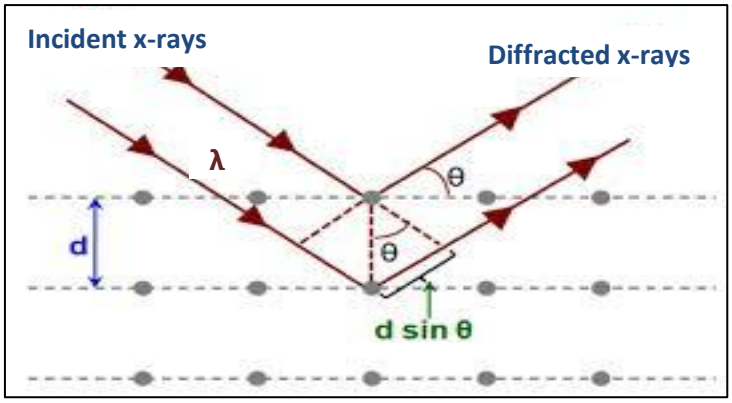

Fig 3.2 Principle of X-ray diffraction analysis [1]

Using X-ray diffraction method we can find out structural information of the material prepared i.e. we can find the nature of sample whether amorphous or crystalline, calculate phase, volume fractions of present phases, crystalline size, lattice parameter and strain in the samples [1].

The present samples were analysed by PANalytical X'Pert PRO diffractometer using Cu K_α radiation (λ=1.54 A°). XRD technique was used to check the nature of the prepared samples, whether they are crystalline or amorphous in nature.

3.2.3 Fourier Transform Infrared Spectroscopy (FTIR)

The main goal of this technique is to find out chemical functional group present in the sample. When the infrared radiations fall on sample, characteristic frequencies are absorbed by different functional groups. The final spectrum displays absorption and transmission by the sample. An IR spectrum for each functional group is different just like the fingerprints [2]. Many types of samples like gases, solids and liquids can be analysed using IR spectrometer. The information about bond strength, transmission, functional group can be directly extracted from the IR spectra. The frequency of absorbed radiations matches the transition energy of the bond or the group that vibrates. Perkin Elmer-Spectrum-RF-1 FTIR spectrometer was used to analyse the samples at room temperature.

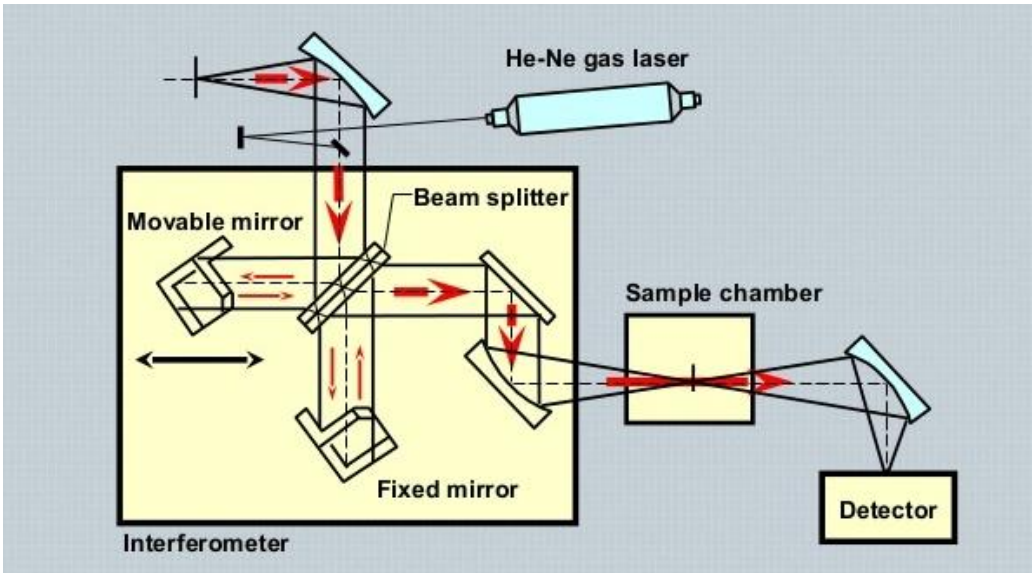

Fig 3.3 Instrumentation of FTIR [6]

3.2.4 UV-Visible spectroscopy

UV-Visible spectroscopy uses light radiations in visible region and adjacent ranges to directly record the absorption or reflectance spectra. Colour of the involved chemical is directly influenced by reflectance or absorbance. In this region the atoms and molecules experience electronic transitions. Absorption spectroscopy and fluorescence spectroscopy are interrelated to each other, as in fluorescence spectroscopy is related to transitions from excited to ground state whereas absorption spectroscopy measures transition from ground state to excited state. This spectroscopy works on the principle that the bonding and non-bonding electrons in molecule are excited after absorbing energy in form of light. The wavelength of the absorbed light will be longer if the electrons are easily excited [3].

Various optical properties for e.g. optical band gap, refractive index, Urbach energy can be accurately calculated using this spectroscopy [4]. Absorbance can be calculated using Beer-Lambert's law. The intensity of light crossing through the sample (I) is measured using UV-Visible spectrophotometer and then compared to the intensity of incident light before passing through sample (I_o). Ratio of these two intensities I and I_o is called transmittance (T) and is measured in terms of percentage transmittance. The relation between absorbance (A) and

transmittance is given below in equation 3.7.

$$A = -\log(\%T/100) \tag{3.7}$$

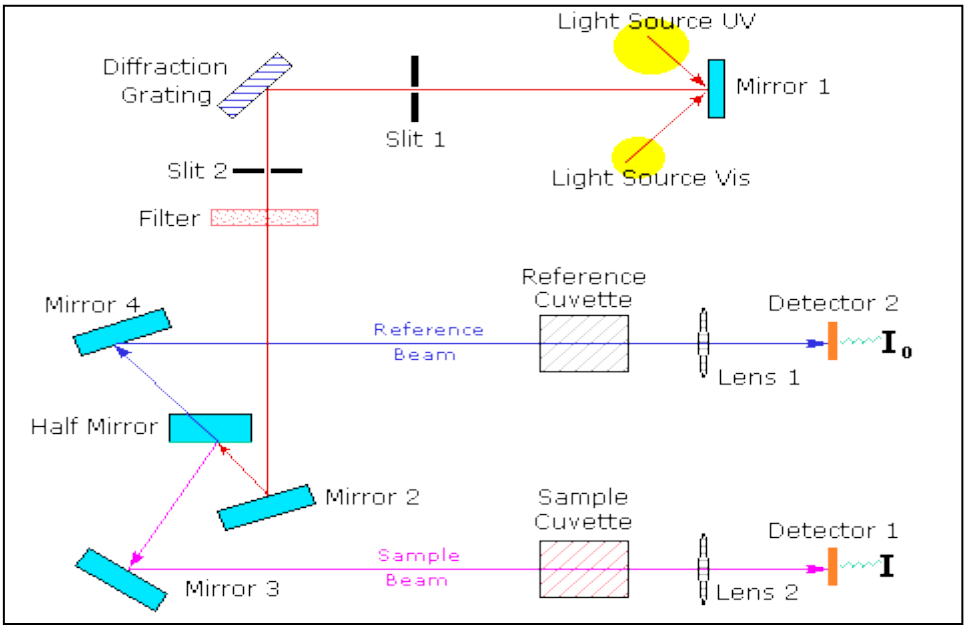

Fig 3.4 Block diagram representing UV-Visible spectrophotometer [6]

The as quenched glass samples were analysed at room temperature using Hitachi U-3900 H double beam spectrophotometer, in the spectral range of 200-800 nm.

3.2.5 Impedance Spectroscopy

The frequency and temperature dependence of electric and dielectric properties of the materials can be studied this technique. From the dielectric constant values as a function of temperature and frequency, various polarization mechanisms (such as space charge, atomic polarisation of dipoles, electronic and orientational polarisation) occuring in the sample can be studied [6]. The real dielectric constant represents the energy stored and the complex dielectric constant represents the dielectric loss in the sysytem. The complex dielectric constant is given as

$$\varepsilon_r = \varepsilon' - i\varepsilon'' \tag{3.8}$$

Where ε' is real permittivity (energy stored in the material), ε'' is imaginary permittivity (dissipation ability of material in electric field) and$i^2 = -1$. Relative loss in the material is

measured as the ratio of imaginary part to real part of permittivity. The Arrhenius plots are obtained between conductivity and temperature to find nature of conduction [5]. The present samples were analysed using Solartron analytical impedance analyzer (Model: SI 1260) at different temperatures and frequencies.

References

1. B.D. Cullity, " Elements of X-ray diffraction", Addison-Wesley Publishing Company, Inc., 2nd edition.
2. F. Daniels, J.W. Willliams, P. Bender, R. A. Alberty, C. D. Cornwell, J. E. Haeeiman, "Experimental Physical Chemistry", 7th edition, McGraw-Hill, New York (1970).
3. T. Owen, "Fundamentals of UV-Visible spectroscopy", A Primer, Agilent Technologies, (2000).
4. H. Kunkely, A. Vogler, J. Inorg. Chem. Commun. 4 (2001) 692.
5. N. Bonanos, P. Pissis, J. R. Macdonald, J. Mater. Charact. 15 (2002) 1.
6. P. Murugasen, S. Sagadevan, D. Shajan, Int. J. Chem. Sci., 13 (2015) 693-713.

4.1 Physical parameters

The obtained physical parameters such as density and molar volume of the as quenched samples are given in Table 4.1. The density and molar volume variation with the different alkali ion is shown in Fig(4.1). It is observed that the density of the Na containing sample is highest as compared to others. As the density is additive property so this trend is caused by the increasing density of alkali oxides present in the samples. K_2O has highest density (2.35g/cc) whereas Li_2O has lowest density (2.01g/cc) amongst these three alkali oxides [1,2]. However, the change in density between Na_2O containing glass and K_2O containing glass is not much. It means that the crosslinking disturbance of glass is less, so packing of different units is not increase too much.

Table 4.1 Density, molar volume, Ionic concentration, Interionic Radii and Polaron radii of the samples

Sample Id	Density (g/cm^3)	Molar Volume (cm^3/mol)	Ionic Concentration ($\times 10^{23}\ cm^{-3}$)	Interionic Radii (A°)	Polaron Radii (A°)
Li20S	2.52	21.35	5.67	1.21	0.48
Na20S	2.58	23.37	5.15	1.24	0.49
K20S	2.60	24.78	4.64	1.28	0.51

The molar volume of the samples increases as the size of the alkali ions increases i.e. the molar volume of Li20S is lowest and that of K20S is highest. This increment in molar volume is attributed to the formation of non-bridging oxygens (NBOs) and lower network connectivity. The ionic concentration (N) and inter-ionic radii (R) are calculated using the following formulae mentioned in previous section.

Fig 4.2 shows the variation in inter-ionic radii along with their ionic concentration as a function of different alkali ion modifier. Evidently, the ionic concentration and their inter-ionic distance show opposite trend. The Li containing sample has highest ionic concentration and lowest inter-ionic radii as compared to others because the covalent character of Li is

more relative to K and Na. Alkali metal oxides are known to modify the glass network. Larger size of the alkali ion leads to creation of more NBOs and more ionic character to the glasses.

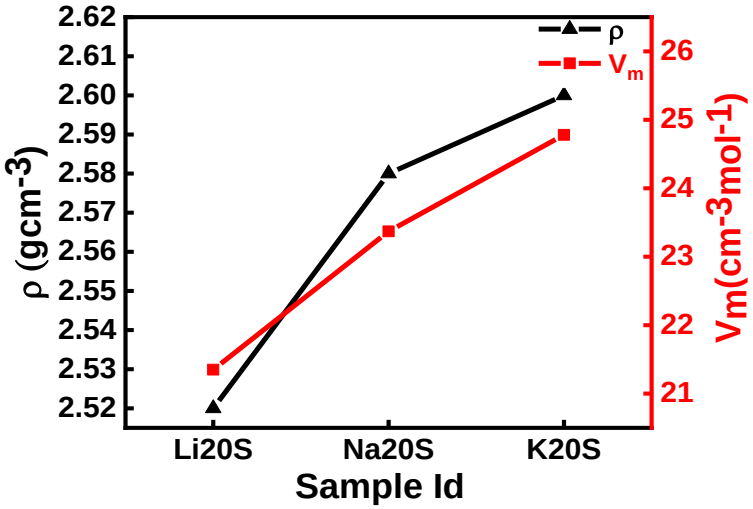

Fig 4.1. Variation in density and molar volume of the glasses

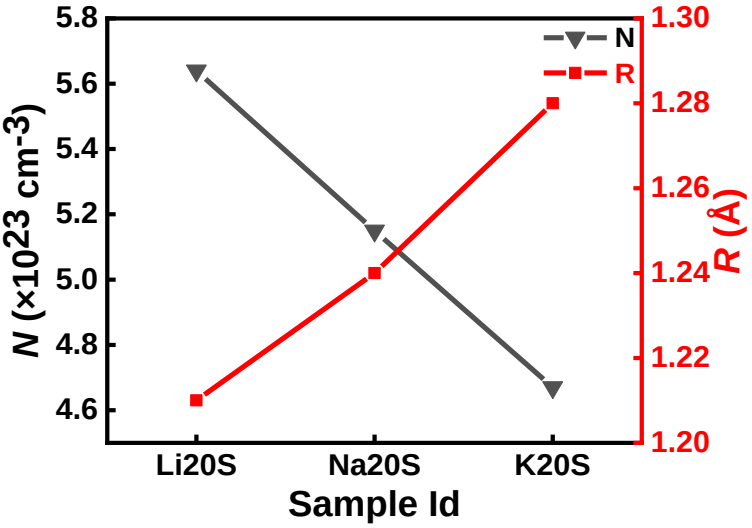

Fig 4.2 Variation in ionic concentration and inter-ionic radii of the glasses

4.2 X-ray diffraction

XRD patterns of the prepared samples are shown in Fig 4.3. Evidently, there are no sharp peaks present in XRD pattern so, the prepared glasses are amorphous in nature. The broad halo is observed between 20° and 30°. It can be clearly seen that, compared to Na20S sample

there is shifting of broad halo in other two samples. For Li20S sample the halo shifts toward lower angle and in case of K20S the halo shifts towards the higher angle. This may be due to the compressive stress present in Li20S sample and the tensile stress in K20S sample as compared to Na20S.

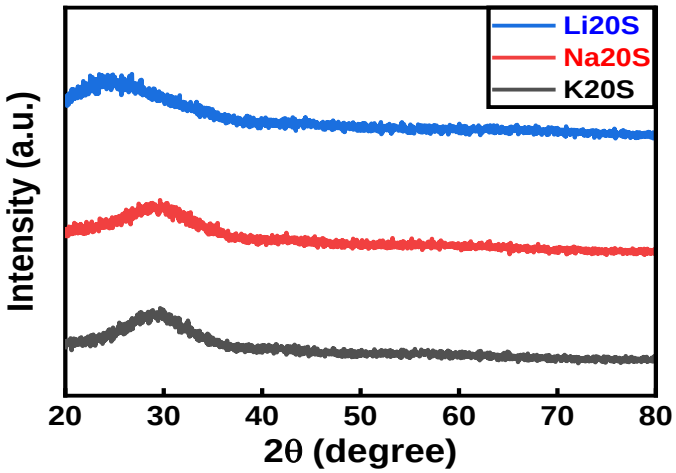

Fig 4.3 XRD patterns of the glass samples

4.3 FTIR spectroscopy

Fig 4.4. shows FTIR spectra of prepared glass samples. These spectra show the transmittance bands at 487 cm^{-1}, 762 cm^{-1}, 941 cm^{-1}, 1028 cm^{-1}, 1425 cm^{-1} and 1630 cm^{-1}. Bands lying between 400-1400 cm^{-1} are present due to the silicate group vibrations with different bonding arrangements and those between 1200-1500cm^{-1} are present due to vibrations of borate network.

Band at 487 cm^{-1} is attributed to bending vibration of SiO_4 tetrahedra [3,4]. The intensity of this absorption band increases with increasing size of the alkali ion present. This may be due to the more ionic bonds which create more of NBO's as the size of alkali ion increases. Also, due to higher field strength of lithium ions, the bond length of Si-O bond increases and hence the bending vibrations decreases. And low field strength of potassium ions leads to more bending vibrations and hence stronger band is observed. The absorption band observed at 762 cm^{-1} is attributed to the Si-O-Si stretching of bridging oxygen [3]. With the substitution of

heavier alkali ion, multiple structural units are created with different bond length between Si-O bond, due to presence of two types of modifier cations (alkali ion and Ca^{2+}) with varied field strength. Hence, as Li^{+} and Ca^{2+} has more difference in their field strength so it results in presence more Si-O units with different bond lengths as compared to K^{+} and Na^{+}. That is why the band for Li20S is broader than other two glasses. The most intense bands at 1028 cm^{-1} and 941 cm^{-1} can be associated with the combined vibrations of the Si-O-Si and B-O-B network of tetrahedra units [3,6,7]. The broadening of the band is due to the overlapping of the vibration modes among different bonds. Also the randomness of glass structure, variations in bond angles, bond length of building units and defects may lead to the band broadening. Band at 1425 cm^{-1} can be assigned to the B-O stretching of the BO_3 units [5,7]. Besides all these bands, band at 1630 cm^{-1} is attributed to the -OH bending mode due to presence of water molecules [3]. A slight shifting of band towards higher or lower wavelength can be seen which may be due to relative change in bond strengths with replacement of different alkali oxides.

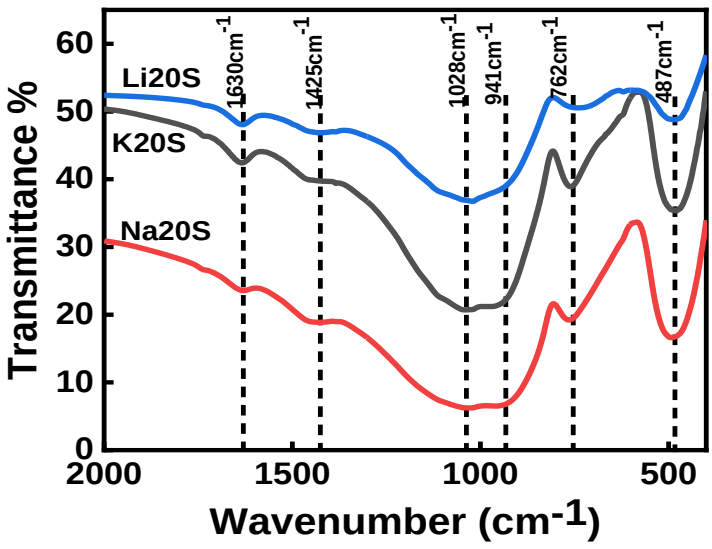

Fig 4.4. FTIR spectra of all the glass samples

4.4 Mechanical properties

Material hardness (H_v) and indentation fracture toughness (K) can be estimated using

Vicker's indentation tests. Vicker's hardness measures the ability of a material to withstand permanent deformation produced by hard material. Vicker's hardness can be calculated by knowing the diagonal length of imprinted indentation (d) and the applied load (F=0.3 Kgf).

$$H_v = 0.18544 \times F/d^2 \quad (4.3)$$

The calculated values of the Vicker's hardness corresponding to the diagonal indentation lengths are given in Table 4.2. As we move from Li to K, the more NBO's are induced in the glass system, as evident from FTIR bands, resulting in change in coordination of boron. As a result the indenter penetrates deeper at a given load. Hence, the hardness of the glass samples decreases with increased penetration depth [8,9]. As ionic bond character increases, the higher atomic number alkali oxide increases the ionic character in the glass which decreases the hardness.

Table 4.2 Calculated values of hardness, elastic modulus and fracture toughness of all samples

Sample Id	Vicker's hardness (HV)	Elastic Modulus (E) GPa	Fracture Toughness (K) MPa $m^{½}$
Li20S	631.07	80.57	--
Na20S	604.32	67.96	0.82
K20S	524.56	65.11	0.80

Fracture toughness (K) is defined as the ability of a material to overcome the fracture. Fracture toughness can be calculated by measuring the crack length (c) generated off the corners of indenter. The fracture toughness (K) can be estimated using half-penny median-radial cracks model [8], and the formula is given as

$$K = 0.016\left(\frac{E}{H}\right)^{\frac{1}{2}}\left(\frac{F}{c^{\frac{3}{2}}}\right) \quad (4.4)$$

where, E is the modulus of elasticity and is calculated using the formulae:

$$E = 2(V_t.G_t) \quad (4.5)$$

where, V_t is the packing density of the glass. Further V_t and G_t values are calculated as:

$$G_t = \sum(x_i \,.\, G_i) \tag{4.6}$$

$$V_i = \frac{4}{3}\pi N_A(x.R_M^3 + y.R_O^3) \tag{4.7}$$

$$V_t = V_M^{-1}\sum(x_i.V_i) \tag{4.8}$$

where, R_M and R_O are the respective Pauling' s ionic radius of metal M and oxygen O, N_A is Avogadro's number, V_M the molar volume of glass, x_i the mole fraction of i^{th} oxide and G_i is dissociation energy per unit volume of the i^{th} oxide [10,12,13].

The calculated values of fracture toughness are mentioned in Table 4.2. It is observed that there is no fracture toughness observed in Li containing sample. This may be due to the reason as the Li20S samples has the highest hardness value, being more brittle in nature there is no crack observed under the applied stress. It clearly indicate that the covalent bond characteristic is higher in this glass than other two glasses.The Na20S has fracture toughness greater than that of K20S, this is attributed to greater bond strength of Na_2O than K_2O and hence Na_2O has greater much attraction between bonds [11]. Similar values of hardness and fracture toughness are observed in studies done before (as discussed in chapter2) [8,9].

4.5 UV-Visible spectroscopy analysis

According to Tauc, relation among absorption coefficient and the photon energy contains three portions. First region is used to measure the optical band gap i.e. Tauc's region which corresponds to high absorption coefficient For Tauc's region, relation among absorption coefficient and the photon energy is discussed by Mott and Davis [11], and is given as:

$$\alpha h\upsilon = A[(h\upsilon - E_g)^n/h\upsilon] \tag{4.9}$$

where, A is proportionality constant, hυ is photon energy and E_g is the optical band gap.

The value of direct optical band gap is calculated by extrapolating the linear region of $(\alpha h\upsilon)^2$ w.r.t $(h\upsilon)$ plot. The x-intercept will give the value of optical band gap. In same way to calculated indirect energy band gap, the x-intercept of linear region of $(\alpha h\upsilon)^{1/2}$ versus $(h\upsilon)$ is calculated. The calculated values of direct band gaps are listed in Table 4.2. It can be clearly

seen that the band gap of glasses lies in insulator range. The K20S glass has highest optical band gap.

Urbach region is the tailing region which is exponential in nature and it corresponds to disordered and disoriented structure of the system [11]. In this region $\alpha(\upsilon)$ depends exponentially on photon energy as follows:

$$\alpha = \alpha_0 \exp\left(h\upsilon/E_u\right) \tag{4.10}$$

where, α_o is constant and E_u is Urbach energy. The reciprocal of the slope of ln(α) versus hυ graph gives the value of Urbach energy.

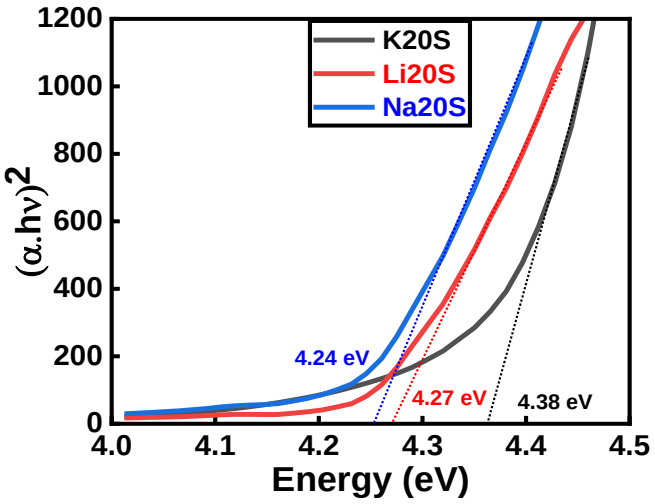

Fig 4.5 Optical band gap of the glass samples

The Urbach energy values are listed in Table 4.3. The Li20S sample has lowest and K20S sample has highest value of Urbach energy. It may be due to presence of more number of NBO's in K20S sample as discussed in previous section. Arya *et al.* [3] studied the optical properties of glasses with composition ((70-*x*)SiO_2-*x*Na_2O-15CaO-10Al_2O_3-5TiO_2, where 10≤*x*≤25). The optical band and Urbach energy values of these glasses were observed to be more than that of glasses being discussed. This is due to different compositions of glasses resulting in different number of NBO's present in glass systems. Compared to glasses

prepared and the glasses studied by Arya and his team, there are more number of NBO's present in later glass system.

Table 4.3 Optical parameters of the glass samples

Sample Id	Optical band gap (eV)	Optical Basicity	Polarisability $(\alpha_m)\times10^{-23}$cc	Urbach energy(eV)
Li20S	4.27	0.582	1.43	0.203
Na20S	4.24	0.600	1.45	0.221
K20S	4.38	0.626	1.49	0.288

4.6 Theoretical optical basicity

Duffy and Ingram proposed the formula for calculating the optical basicity ($\wedge_m$) given by equation 4.11. The term optical basicity refers to the tendency of oxygen atoms to transfer a part of negative charge to the surrounding ions. The optical basicity values for the three glass samples are given in Table 4.3.

$$\wedge_m = \Sigma O_i / O\gamma_m \tag{4.11}$$

Where, O is the total number of oxygen atoms, γ_m is the basicity moderating parameter and O_i is the number of individual atoms present in oxides. Therefore, for the three glass samples the optical basicity ($\wedge_m$) can be calculated as given in equation 4.12.

$$\wedge_m = \frac{1}{O}\left[\frac{O_i(SiO_2)}{\gamma_m(SiO_2)} + \frac{O_i(B_2O_3)}{\gamma_m(B_2O_3)} + \frac{O_i(CaO)}{\gamma_m(CaO)} + \frac{O_i(X_2O)}{\gamma_m(X_2O)}\right] \tag{4.12}$$

(Where X=Li, Na, K).

It is noticed that the optical basicity of glasses with Li ions is least and that with K ions is the highest. This is due to the reason that as the size of the alkali ions increases the NBO's in the glass system increases and hence the optical basicity increases [11].

4.7 Oxide ion polarisability

Oxide ion polarisabiltiy (α_o) is strongly related to the optical basicity. Increase in oxide ion polarisability indicates the stronger ability of oxide ions to transfer the negative charge [11]. To calculate the oxide ion polarisability, Duffy gave the following equation

$$\alpha_o = [(1.567\wedge_m + 0.362)^2 + 2.868]/3.133 \quad (4.13)$$

It is clearly seen that the oxide ion polarisability and optical basicity are directly related to each other. The α_o values of the three glass samples are mentioned in Table 4.3. The K20S glass has the highest value of oxide ion polarisability and optical basicity also. This means that K20S glass oxide ions have more electron donating ability as compared to other two glasses.

4.8 Dielectric properties

The dielectric properties of glasses arise due to different polarisation mechanisms (electronic, ionic, orientational and space charge polarisation). The dielectric permittivity of the glass samples is expressed as:

$$\varepsilon_r(w) = \varepsilon_r'(w) - i\varepsilon_r''(w) \quad (4.14)$$

where $\varepsilon_r'(w)$ represents the real part of dielectric permittivity which gives information about the energy stored in the system, $\varepsilon_r''(w)$ represents the imaginary part of the dielectric permittivity (dielectric loss), w is the angular frequency.

Fig 4.6 shows the variation of dielectric constant with frequency at different temperatures (in °C) for all the three samples. It is clear from Fig 4.6 that dielectric constant remains almost frequency independent at lower temperatures up to 300°C, and increases sharply at lower frequencies, beyond 400°C. As the temperature increases, mobility of alkali ions increases. It is found that the ε' values for Li20S sample is higher than that of K20S and Na20S glasses. This is because of higher mobility of lithium ions leading to more hopping of Li^+ ions. At low frequencies the ε' variation is due to the contribution of deformational (ionic and electronic) and relaxational (orientational and interfacial) polarisations [14,15]. The decrease in ε' value at high frequency can be attributed to orientational polarisation because relative to ionic and electronic polarisation, orientational polarisation takes more time and decreases with frequency [14]. The decrease in dielectric values with frequency is also evident from Fig 4.7.

The variation of dielectric constant with temperature at different frequencies is shown in Fig 4.7. The dielectric values remain constant upto 300°C and then increases with increasing temperature. Space charge polarisation and orientation polarisation both strongly depend upon temperature, but in opposite manner i.e. space charge polarisation increases with temperature whereas orientation polarisation decreases with temperature. Hence, increase in dielectric constant with temperature is dominated by space charge polarisation [16,18].

As observed from Fig 4.6, lithium containing glass has highest and potassium containing sample has lowest value of dielectric constant. Similar dielectric characteristics were reported by Wang and his team in 2008 [16].

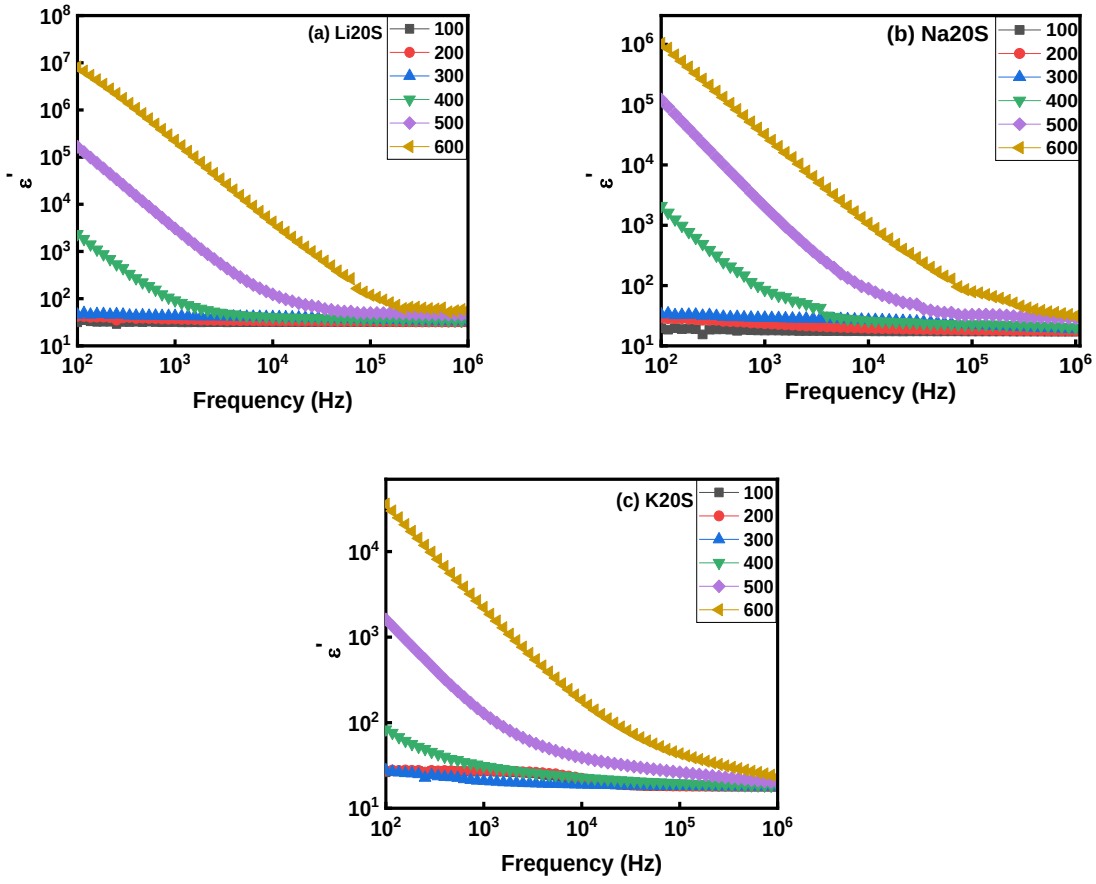

Fig 4.6 Change in dielectric constant with frequency at different temperatures (°C) for (a) Li20S (b) Na20S and (c) K20S glass samples

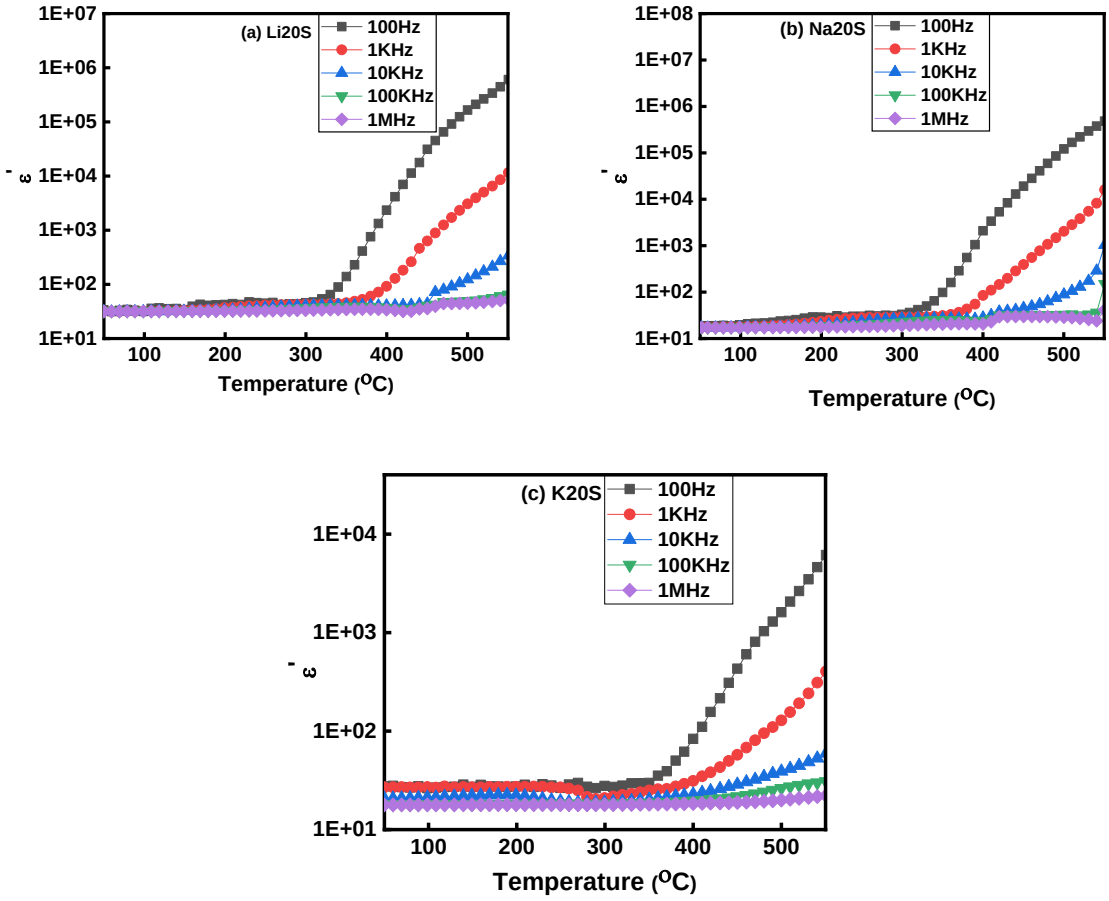

Fig 4.7 Change in dielectric constant with temperature for all the glass samples

4.10 Tangent of losses

Fig 4.8 (a)-(c) s hows the variation of tanδ w.r.t. frequency at different temperatures for all the three samples. It may be clearly noted that for Li20S glass, relaxation effects are only visualised for temperatures above 300°C and for K20S sample relaxation effects are present for temperature above 400°C. It may be noted that as temperature increases, relaxation peaks shifts towards the higher frequency. In present case, the dielectric relaxation corresponds to migration of alkali ions across the interstitial sites in glass matrix. According to Maxwell's theory, the relaxation peaks may be present due to trapping of conducting ions in less conducting glass matrix [19,20]. Hence relaxation peaks corresponds to conduction process of alkali ions. The tangent of loss increases with increasing temperature which may be due to thermal agitations

which affects the re-orientation of dipoles along the direction of electric field [14,21]. At low temperatures there are no relaxation peaks present because there is no trapping of alkali ions in the glass matrix.

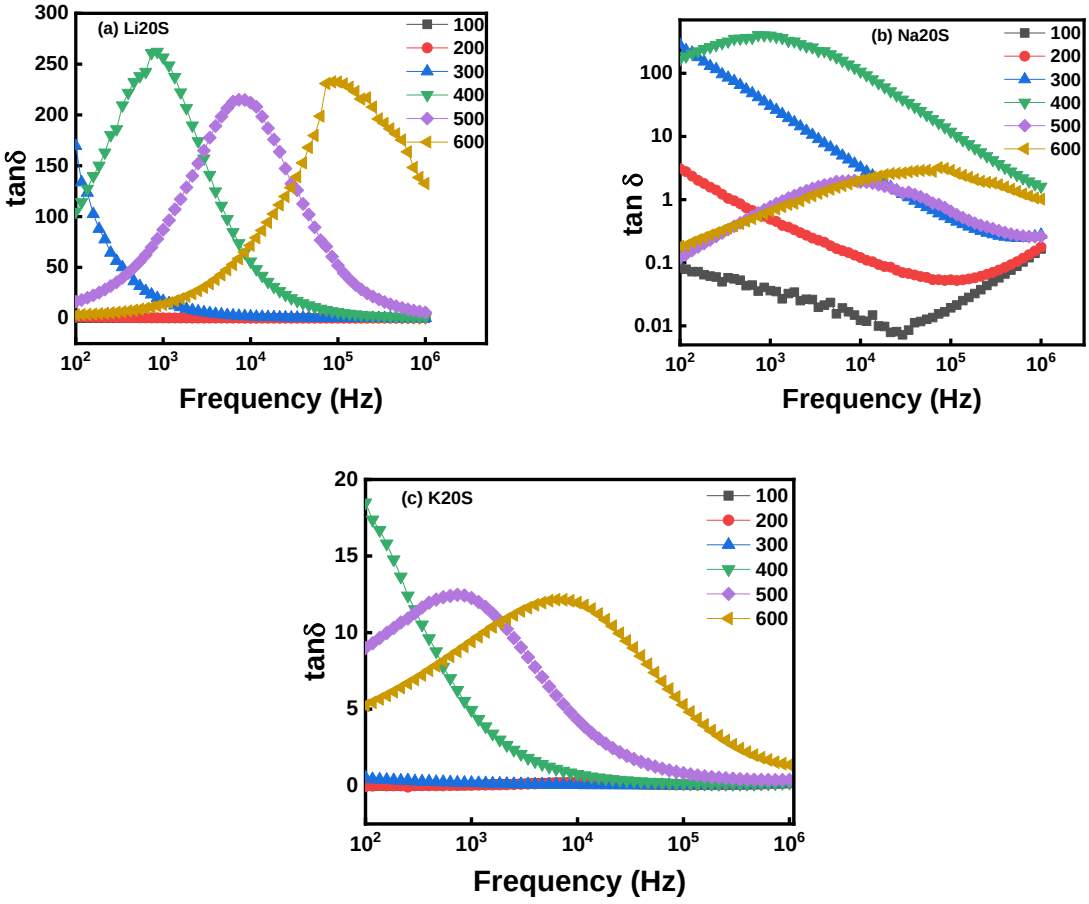

Fig 4.8 Variation of tangent of loss with frequency at different temperature of all samples

4.11 Conductivity analysis

The change in conductivity for all three glass samples with respect to frequency at different temperatures has been plotted and shown in Fig4.9 (a)-(c). The conductivity curve consists of two regions, the one with frequency independent curve that is known as plateau region at lower frequency which attributes to long range migration of ions and the second region which corresponds to ac conductivity [14]. The frequency dependent conductivity follows Jonscher's power law given by equation 4.15

$$\sigma_\omega = \sigma_0 + A\omega^s \qquad (4.15)$$

where, σ_o is the dc conductivity, which is frequency independent, ω is the angular frequency, A is pre-exponential factor and *s* is power law exponent. The term $A\omega^s$ represents the dispersive component of ac conductivity.

It may be noted that for all three samples, at low temperature and high frequency the conductivity increases sharply. In case of alkali oxides, the hopping of charge carriers from one site to other nearest neighbouring site is responsible for ac conductivity [14]. The low frequency plateau region corresponds to dc conductivity of the glasses. It is observed that the dc conductivity increases directly with temperature. DC conductivity is thermally activated phenomenon. The ac conductivity and dc conductivity follows same trend. The Li20S has highest value of dc conductivity, this may be due to higher ionic concentration and higher mobility of Li^+ ions.

Activation energy of the samples is calculated from Arrhenius plots for thermally activated conduction mechanism given as follows

$$\sigma = \sigma_0 \exp\left[\frac{-E_a}{k_B T}\right] \tag{4.16}$$

where, E_a is the activation energy for conduction, T is absolute temperature and k_B is the Boltzmann constant. The values of activation energies for all samples are listed in Table 4.4

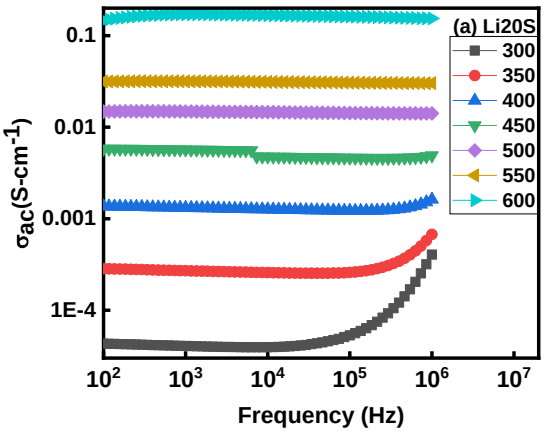

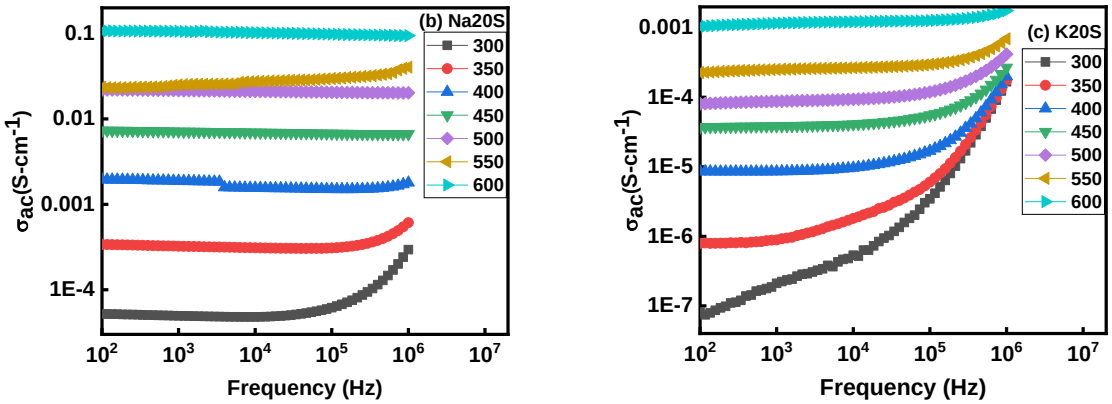

Fig 4.9 Frequency dependence of conductivity for (a) Li20S, (b) Na20S and (c) K20S samples at different temperatures (°C)

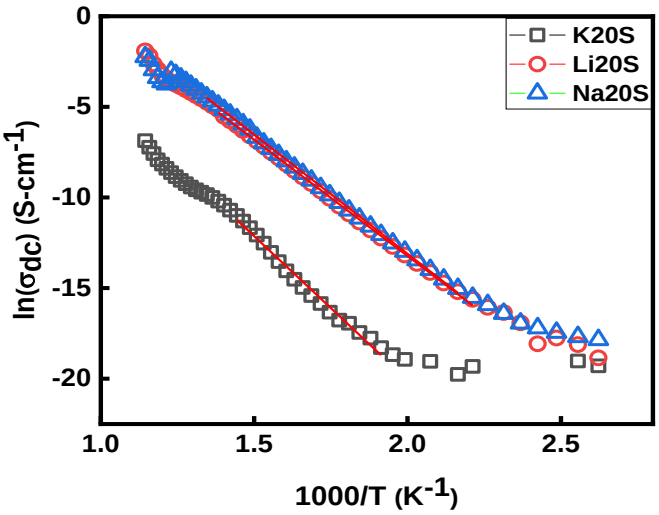

Fig 4.10 Arrhenius plot for all glass samples

Table 4.4 Activation energy and dc conductivity (at 400°C) values of all three samples

Sample Id	Temperature range (°C)	Activation Energy (E_a)	DC conductivity values (S/cm^{-1})
Li20S	180-440	1.11	0.00195
Na20S	190-470	1.13	0.00137
K20S	250-410	1.43	8.58×10^{-6}

It is clear that K20S has highest and the sample Li20S has least value of activation energy. As discussed above the conductivity of sample with Li^+ ions is more that means they are

more mobile than other two and this conductivity variation supports the activation energy value of Li20S. This shows that among different alkali ions, Li ions have the highest tendency to conduct, while Na ions are also comparable. K ions have the least potential towards conductivity in the glass network, owing to their higher ionic radii. Neyret *et al* [22] showed the similar trend in activation energy with different alkali ions present in the glasses. Also he showed that independent of alkali ion present, conductivity of glasses follow the Arrhenius law.

References

1. Pradyot Patnaik. Handbook of Inorganic Chemicals. McGraw-Hill, 2002.
2. Wells, A.F. (1984) Structural Inorganic Chemistry, Oxford: Clarendon Press.
3. S.Arya, B.Kaur, G.Kaur *et al.*, J. Therm Anal Calorim, 120 (2015) 1163-1171.
4. S.A. Macdonald, C.R. Shardt, D.J. Masiello, *et al.* , J. Non-Cryst Solids, 275 (2000) 72-82.
5. A.W. Beckmann, D. Moncke, D. Palles, *et al*, J. Non-Cryst Solids, 405 (2014) 196-206.
6. V. Naresh, S. Buddhudu, Ceram. Int., 38 (2012) 2325-2332.
7. N. Hanumantharaju, G. Sriprakash, V. Gowda, J. Non-Cryst Solids, 52 (2019) 103-111.
8. M. Salinigopal, N. Gopakumar, P. Anjana, Silicon, (2019).
9. M. Barlet, J. Delaye, T. Charpentier *et al.*, J. Non-Cryst Solids, 417-418 (2015) 66-79.
10. M. Smedskjaer, M. Jensen, Y. Yue, J. Non-Cryst Solids, 356 (2010) 893-897.
11. D. Souri, Measurement, 44 (2011) 1904-1908.
12. G. Kaur, O.P. Pandey, K. Singh, J. Non-Cryst Solids, 358 (2012) 2589-2596.
13. A. Makishima, J.D. Mackenzie, J. Non-Cryst Solids, 12 (1973) 35-45.
14. A. Makishima, J.D. Mackenzie, J. Non-Cryst Solids, 17 (1975) 147-157.
15. N. Hanumantharaju, G. Sriprakash, V. Gowda, J. Non-Cryst Solids, 512 (2019) 103-111.
16. M. Barssoum, Fund. Ceram, McGraw Hill, New York, 1977.
17. Z. Wang, Y. Hu, H. Lu *et al.*, J. Non-Cryst Solids, 354 (2008) 1128-1132.
18. J. Serra, P. Gonzalez, S. Liste *et al.*, J. Non-Cryst Solids, 332 (2003) 20-27.
19. S. Khan, G. Kaur, K. Singh, Ceram. Int., 43 (2017) 722-727.
20. N. Bansal, G. Kaur, K. Singh, Mater. Res. Bull., 98 (2018) 34-40.
21. P. Singh, A. Agarwal, S. Sanghi, *et al.*, Ceramics Phys. B 436 (2014) 64–73.
22. S. Yusub, P.S. Rao, D.K. Rao, J. Alloys Compd. 663 (2016) 708–717.
23. M. Neyret, M. Lenoir, A. Grandjean *et al.*, J. Non-Cryst Solids, 410 (2015) 74-81.

Chapter-5 Conclusion and Future Scope of the work

Different alkali oxide containing glasses are synthesised by melt quench technique. The density increases as atomic weight increases of substituted alkali metal oxides. The ionicity of the glasses increases as Li_2O is replaced by Na_2O and K_2O in the glass composition. On the other hand, the hardness and elastic modulus decreases from Li_2O to K_2O containing glasses. From FTIR spectra, it is observed that as Li_2O is replaced with K_2O the bands become stronger. As the size of alkali ion increases in the glass, the tendency of oxide ions to donate electron also increases. The optical band gap of glasses lies in insulator range i.e. from 4.27 eV – 4.38 eV. Activation energy of glasses lies from 1.11 eV to 1.43 eV. Li20S glass has the highest value of ionic concentration and lowest interionic radii. The highest conductivity is observed in Li20S glass.

Future scope of the work:

The present glasses can be further characterized to study the thermal properties using TG-DTA and dilatometry for possible application as substrate in thin film solar cells. The diffusion kinetics of alkali ions from substrate to the overlayers of solar cell can be performed to check their suitability as a substrate for Cu_2ZnSnS_4 thin film solar cell.

Turnitin Originality Report

Processed on: 15-Jul-2019 12:56 +0530
ID: 1152006407
Word Count: 7494
Submitted: 1

rajni gupta thesis v03 By Rajni Gupta

Similarity Index	Similarity by Source	
13%	Internet Sources:	1%
	Publications:	8%
	Student Papers:	12%

1% match (student papers from 13-Jul-2018)
Class: MSc Thesis 2018
Assignment: MSc Thesis 2018
Paper ID: 982260569

1% match (student papers from 13-Jul-2018)
Class: MSc Thesis 2018
Assignment: MSc Thesis 2018
Paper ID: 982256973

1% match (student papers from 01-Aug-2016)
Class: Thesis
Assignment: Thesis July 2016 - July 2017
Paper ID: 693069348

1% match (publications)
Savidh Khan, G. Kaur, K. Singh. "Effect of ZrO2 on dielectric, optical and structural properties of yttrium calcium borosilicate glasses", Ceramics International, 2017

1% match (student papers from 07-Apr-2016)
Class: Thesis
Assignment: Thesis 2015
Paper ID: 655787713

1% match (student papers from 14-Jul-2016)
Class: Thesis
Assignment: Thesis 2015
Paper ID: 689573106

1% match (publications)
S.K. Arya, G. Kaur, K. Singh. "Effect of vanadium on the optical and physical properties of lithium borate glasses", Journal of Non-Crystalline Solids, 2016

< 1% match (publications)
Satwinder Singh, K. Singh. "Nanocrystalline glass ceramics: Structural, physical and optical properties", Journal of Molecular Structure, 2015

< 1% match (publications)
Marina Barlet, Jean-Marc Delaye, Thibault Charpentier, Mickael Gennisson, Daniel Bonamy, Tanguy Rouxel, Cindy L. Rountree. "Hardness and toughness of sodium borosilicate glasses via Vickers's indentations", Journal of Non-Crystalline Solids, 2015

< 1% match (student papers from 12-Jul-2018)
Class: MSc Thesis 2018
Assignment: MSc Thesis 2018
Paper ID: 982048598

< 1% match (publications)
Sanjay Gopal Ullattil, Pradeepan Periyat, Binu Naufal, Manoj Ainikalkannath Lazar. "Self-Doped ZnO Microrods—High Temperature Stable Oxygen Deficient Platforms for Solar Photocatalysis", Industrial & Engineering Chemistry Research, 2016

< 1% match (publications)
Awadhesh Kumar Yadav, Priyanka A. Jha, Sevi Murugavel, Prabhakar Singh. "Synthesis, characterization and AC conductivity of alkali metal substituted telluride glasses", Solid State Ionics, 2016

< 1% match (publications)
A. Abd El-Moneim. "Ultrasonic and structural studies on TiO2-doped CaO–Al2O3–B2O3 glasses", physica status solidi (a), 09/2003

< 1% match (publications)
Mandeep Kaur, Gurbinder Kaur, V. Kumar. "Influence of intermediates on the optical and theoretical parameters of xLa2O3-(10-x) Y2O3 -15SrO-15CaO -10B2O3-10Al2O3-40SiO2 (2 ≤ x ≤ 8) glasses", Journal of Non-Crystalline Solids, 2018

< 1% match (publications)
Praveen Jha, K. Singh. "Effect of Field Strength and Electronegativity of CaO and MgO on Structural and Optical Properties of SiO2–K2O-CaO-MgO Glasses", Silicon, 2015

< 1% match (Internet from 15-Dec-2018)
http://publications.thapar.edu/index.php?s_in=j_year&s_text=2015

< 1% match (student papers from 21-Aug-2018)
Submitted to Osmania University, Hyderabad on 2018-08-21

< 1% match (student papers from 28-Jun-2018)
Submitted to Universiti Teknologi Malaysia on 2018-06-28

< 1% match (student papers from 25-Dec-2016)
Submitted to Mansoura University on 2016-12-25